

Supporting Information

Luminescence spectra simulation of Ce³⁺-activated phosphors by accumulating emission lines along first-principles molecular dynamics trajectories

Satoru Matsuishi¹, Hidekazu Ikeno, Yukinori Koyama, and Takashi Takeda

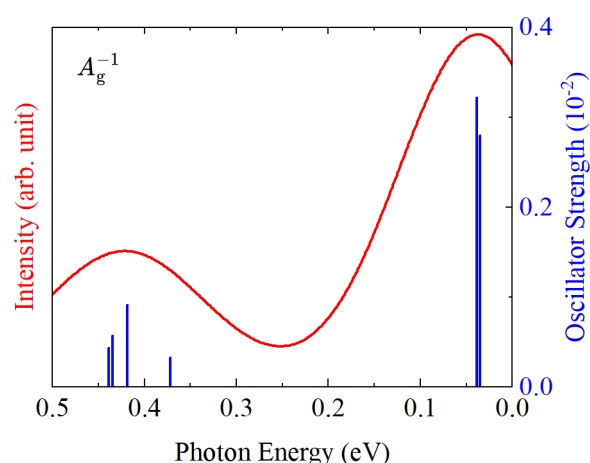


Figure S1. Calculated absorption spectra of YAG:Ce structure model (red curve) using TDM from the lowest Ce 4f level to higher levels in A_g^{-1} states. Blue bars indicate the calculated transition energies and the oscillator strengths.

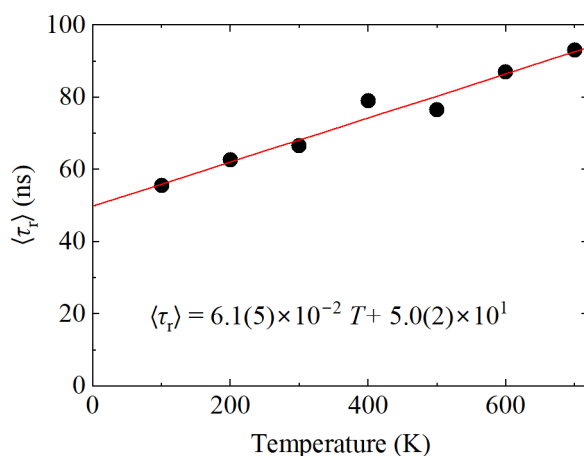


Figure S2. Average radiative lifetime $\langle \tau_r \rangle$ as a function of temperature calculated along the trajectory of FPMD for YAG:Ce structure model.

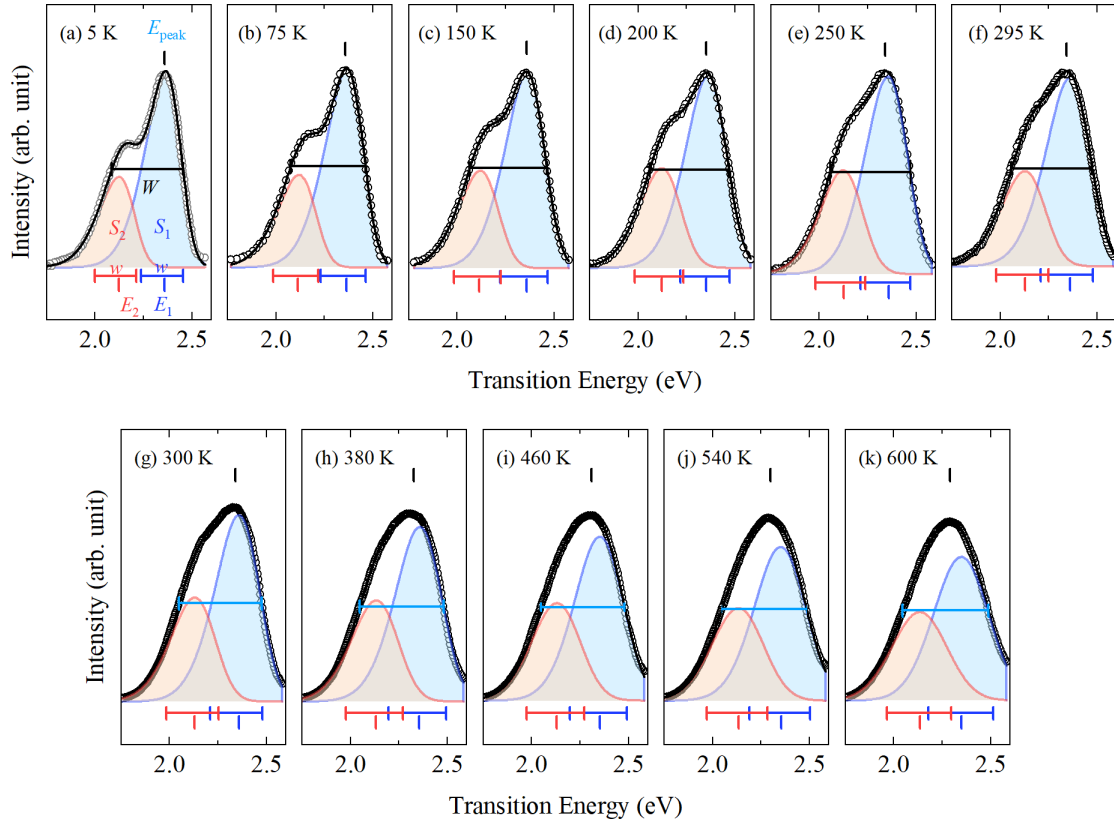


Figure S3. Evaluation of emission peak positions and FWHMs in experimental luminescence emission spectra of YAG:Ce at 5-600 K taken from literature.^[S1] The spectral intensity $\rho(\lambda)$ in the wavelength domain was converted to the spectral intensity $\rho(\epsilon)$ in the energy domain by the equation $\rho(\epsilon) = (\lambda^2/hc) \rho(\lambda)$. In the reference, the YAG:Ce luminescence spectra were measured below 295 K and above 300 K using different spectrophotometers. Because the sensitivity curves of the two spectrometers are different, the spectra above 300 K were corrected using the intensity ratio of the spectra at 300 K and 295 K; $\rho_{\text{corr}}(\epsilon) = \rho_{294}(\epsilon) / \rho_{300}(\epsilon) \rho(\epsilon)$.

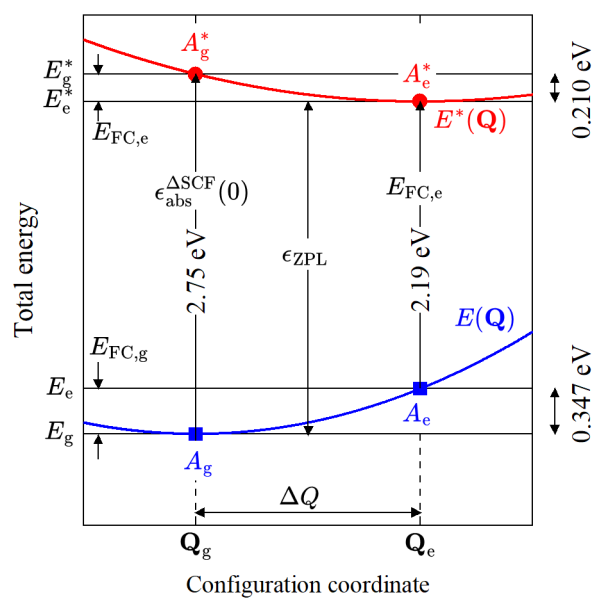


Figure S4. Configuration coordinate diagram of total energy for the $\text{CeY}_{23}\text{Al}_{40}\text{O}_{96}$ structure model obtained by the ΔSCF approach.

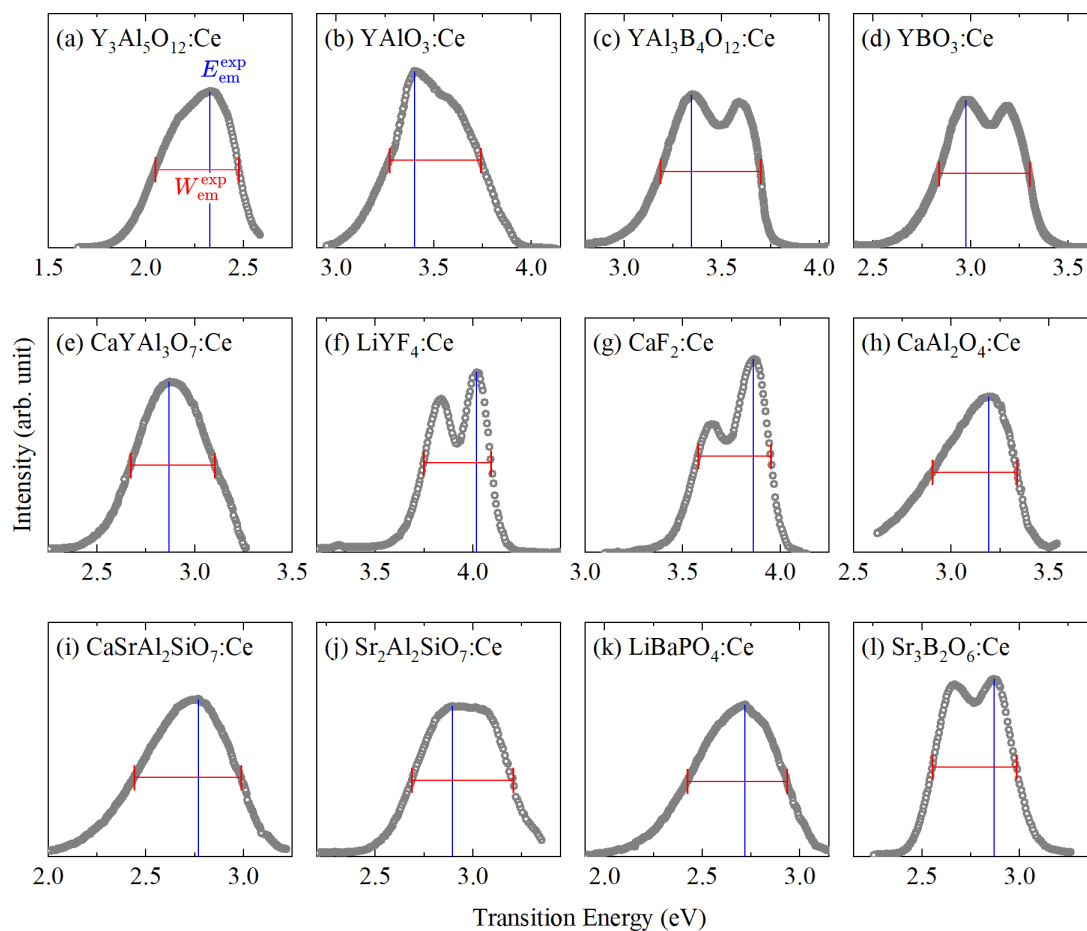


Figure S5. Evaluation of emission peak positions and FWHMs in experimental luminescence emission spectra of 12 known Ce^{3+} -activated phosphors measured at 300 K, taken from the literature. (a) $\text{Y}_3\text{Al}_5\text{O}_{12}:\text{Ce}$,^[S1] (b) $\text{YAlO}_3:\text{Ce}$,^[S2] (c) $\text{YAl}_3\text{B}_4\text{O}_{12}:\text{Ce}$,^[S3] (d) $\text{YBO}_3:\text{Ce}$,^[S3] (e) $\text{CaYAl}_3\text{O}_7:\text{Ce}$,^[S4] (f) $\text{LiYF}_4:\text{Ce}$,^[S5] (g) $\text{CaF}_2:\text{Ce}$,^[S6] (h) $\text{CaAl}_2\text{O}_4:\text{Ce}$,^[S7] (i), $\text{CaSrAl}_2\text{O}_7:\text{Ce}$,^[S8] (j), $\text{Sr}_2\text{Al}_2\text{O}_7:\text{Ce}$,^[S9] (k) $\text{LiBaPO}_4:\text{Ce}$,^[S10] and (l) $\text{Sr}_3\text{B}_2\text{O}_6:\text{Ce}$,^[S11].

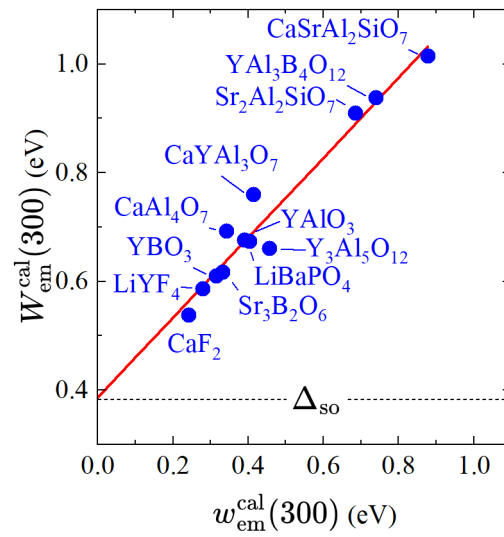


Figure S6. Relation between the FWHM $W_{\text{em}}^{\text{cal}}$ of whole emission band and the FWHMs $w_{\text{em}}^{\text{cal}}$ of $5d_1 \rightarrow {}^2F_{5/2}$ and $5d_1 \rightarrow {}^2F_{7/2}$ bands in the spectra at 300 K in the Ce^{3+} -activated phosphor series.

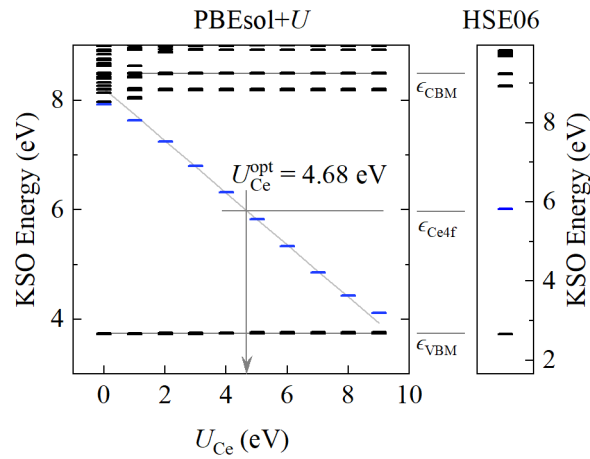


Figure S7. KSO energies as functions of U_{Ce} obtained by PBEsol+ U calculation for $\text{CeY}_{23}\text{Al}_{40}\text{O}_{96}$ model, compared with KSO energies calculated by HSE06 hybrid functional.

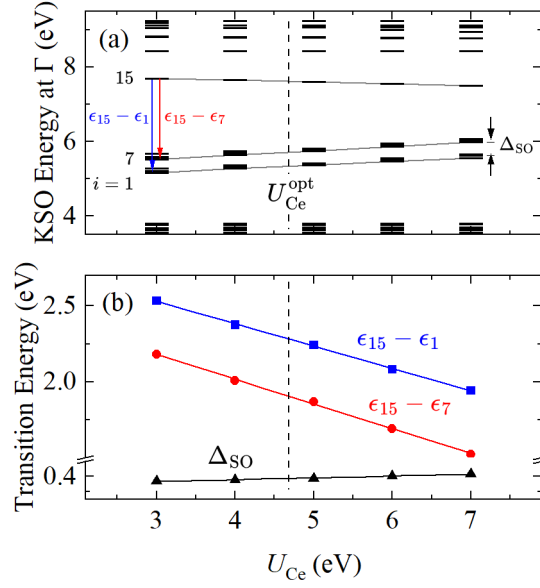


Figure S8. (a) KSO energies at Γ , (b) $\epsilon_{15} - \epsilon_1$ and $\epsilon_{15} - \epsilon_7$ transition energies and spin-orbit splitting Δ_{SO} for A_e^{-1} state in YAG:Ce model as a function of U_{Ce} .

Table S1. List of Ce^{3+} -activated phosphor systems with $U_{\text{Ce}}^{\text{opt}}$ used for structure optimization and total energy calculation and ΔSCF parameters, absorption energy at 0 K ($\epsilon_{\text{abs}}^{\Delta\text{SCF}}(0)$, eV), emission energy at 0 K ($\epsilon_{\text{em}}^{\Delta\text{SCF}}(0)$, eV), Stokes shift at 0 K ($\Delta S(0)$, eV) Franck–Condon shifts for GS ($E_{\text{FS,g}}$) and ES ($E_{\text{FS,e}}$) electronic states, and total normal coordinate change (ΔQ , $\text{amu}^{1/2}\text{\AA}$).

Compounds	$U_{\text{Ce}}^{\text{opt}}$	$\epsilon_{\text{abs}}^{\Delta\text{SCF}}(0)$	$\epsilon_{\text{em}}^{\Delta\text{SCF}}(0)$	$\Delta S(0)$	$E_{\text{FS,g}}$	$E_{\text{FS,e}}$	ΔQ
$\text{Y}_3\text{Al}_5\text{O}_{12}:\text{Ce}$	4.68	2.751	2.194	0.557	0.347	0.210	1.423
$\text{YAlO}_3:\text{Ce}$	3.83	4.114	3.672	0.442	0.285	0.157	1.231
$\text{YAl}_3\text{B}_4\text{O}_{12}:\text{Ce}$	3.51	4.045	3.126	0.919	0.701	0.218	2.026
$\text{YBO}_3:\text{Ce}$	3.77	3.646	3.211	0.435	0.263	0.172	1.132
$\text{CaYAl}_3\text{O}_7:\text{Ce}$	3.84	3.466	2.352	1.114	0.768	0.347	1.473
$\text{LiYF}_4:\text{Ce}$	3.71	4.642	4.485	0.157	0.087	0.070	0.226
$\text{CaF}_2:\text{Ce, F}$	3.40	4.180	3.993	0.187	0.106	0.081	0.895
$\text{CaAl}_4\text{O}_7:\text{Ce, Na}$	3.61	4.089	3.067	1.022	0.693	0.329	2.188
$\text{CaSrAl}_2\text{SiO}_7:\text{Ce, Na}$	3.61	3.799	2.703	1.096	0.821	0.275	1.626
$\text{Sr}_2\text{Al}_2\text{SiO}_7:\text{Ce, Na}$	3.73	3.702	2.810	0.892	0.632	0.261	2.179
$\text{LiBaPO}_4:\text{Ce, Na}$	3.50	4.264	3.581	0.683	0.390	0.294	2.349
$\text{Sr}_3\text{B}_2\text{O}_6:\text{Ce, Na}$	3.53	3.558	2.943	0.615	0.358	0.256	2.514

Table S2. Parameters obtained by harmonic oscillator model analysis of Δ SCF data: Associated effective vibrational energies for GS ($\hbar\Omega_g$, meV) and ES ($\hbar\Omega_e$, meV) electronic states, Huang-Rhys parameters for GS (S_g) and ES (S_e) states, emission energy at 300 K ($\epsilon_{em}^{\Delta SCF}(300)$, eV) and FWHM of emission peak at 300 K ($w_{em}^{\Delta SCF}(300)$, eV).

System	$\hbar\Omega_g$	$\hbar\Omega_e$	S_g	S_e	$\epsilon_{em}^{\Delta SCF}(300)$	$w_{em}^{\Delta SCF}(300)$
Y ₃ Al ₅ O ₁₂ :Ce	37.8	29.4	9.17	7.13	2.265	0.426
YAlO ₃ :Ce	39.6	29.4	7.19	5.34	3.722	0.405
YAl ₃ B ₄ O ₁₂ :Ce	37.8	21.1	18.55	10.35	3.332	0.826
YBO ₃ :Ce	41.4	33.5	6.35	5.14	3.251	0.362
CaYAl ₃ O ₇ :Ce	54.4	36.6	14.12	9.49	2.533	0.752
LiYF ₄ :Ce	119.3	107.0	0.73	0.65	4.496	0.257
CaF ₂ :Ce,F	33.3	29.1	3.19	2.79	4.008	0.209
CaAl ₄ O ₇ :Ce,Na	34.8	24.0	19.92	13.73	3.194	0.669
CaSrAl ₂ SiO ₇ :Ce,Na	50.9	29.5	16.12	9.33	2.942	0.882
Sr ₂ Al ₂ SiO ₇ :Ce,Na	33.4	21.4	18.95	12.18	2.959	0.681
LiBaPO ₄ :Ce,Na	24.3	21.1	16.05	13.93	3.619	0.396
Sr ₃ B ₂ O ₆ :Ce,Na	21.8	18.4	16.45	13.91	2.989	0.387

Table S3. Peak energies ($\epsilon_{5/2}^{\text{cal}}$ and $\epsilon_{7/2}^{\text{cal}}$, eV), SO splitting ($\Delta_{\text{SO}}^{\text{cal}}$, eV), FWHMs ($w_{5/2}^{\text{cal}}$ and $w_{7/2}^{\text{cal}}$, eV) and areal intensity ratio ($s_{7/2}^{\text{cal}}/s_{5/2}^{\text{cal}}$) of $5d_1 \rightarrow {}^2F_{5/2}$ and $5d_1 \rightarrow {}^2F_{7/2}$ emission bands from peak fitting for emission spectra obtained by FPMD spectra accumulation method $I_{5/2}(\epsilon)$ and $I_{7/2}(\epsilon)$ at 300 K.

System	$\epsilon_{5/2}^{\text{cal}}$	$\epsilon_{7/2}^{\text{cal}}$	$\Delta_{\text{SO}}^{\text{cal}}$	$w_{5/2}^{\text{cal}}$	$w_{7/2}^{\text{cal}}$	$s_{7/2}^{\text{cal}}/s_{5/2}^{\text{cal}}$
$\text{Y}_3\text{Al}_5\text{O}_{12}:\text{Ce}$	2.226	1.856	0.370	0.455	0.458	0.524
$\text{YAlO}_3:\text{Ce}$	3.512	3.132	0.380	0.388	0.393	0.627
$\text{YAl}_3\text{B}_4\text{O}_{12}:\text{Ce}$	3.196	2.816	0.380	0.750	0.731	0.599
$\text{YBO}_3:\text{Ce}$	3.269	2.898	0.371	0.314	0.316	0.636
$\text{CaYAl}_3\text{O}_7:\text{Ce}$	2.578	2.198	0.380	0.491	0.482	0.630
$\text{LiYF}_4:\text{Ce}$	4.648	4.278	0.370	0.279	0.280	0.642
$\text{CaF}_2:\text{Ce},\text{F}$	4.375	4.005	0.370	0.243	0.243	0.602
$\text{CaAl}_4\text{O}_7:\text{Ce},\text{Na}$	2.918	2.528	0.390	0.360	0.337	0.707
$\text{CaSrAl}_2\text{SiO}_7:\text{Ce},\text{Na}$	2.813	2.443	0.370	0.885	0.875	0.659
$\text{Sr}_2\text{Al}_2\text{SiO}_7:\text{Ce},\text{Na}$	3.187	2.817	0.370	0.670	0.712	0.667
$\text{LiBaPO}_4:\text{Ce},\text{Na}$	3.374	2.924	0.450	0.384	0.399	0.526
$\text{Sr}_3\text{B}_2\text{O}_6:\text{Ce},\text{Na}$	2.910	2.530	0.380	0.334	0.333	0.576

Table S4. Peak energy ($E_{\text{em}}^{\text{cal}}$, eV) and FWHM ($W_{\text{em}}^{\text{cal}}$, eV) of calculated whole emission spectrum $I(\epsilon)$ at 300 K compared with their experimental values ($E_{\text{em}}^{\text{exp}}$ and $W_{\text{em}}^{\text{exp}}$, eV) taken from literature.

System	$E_{\text{em}}^{\text{cal}}$	$W_{\text{em}}^{\text{cal}}$	$E_{\text{em}}^{\text{exp}}$	$W_{\text{em}}^{\text{exp}}$
$\text{Y}_3\text{Al}_5\text{O}_{12}:\text{Ce}$	2.186	0.660	2.339	0.427
$\text{YAlO}_3:\text{Ce}$	3.492	0.676	3.455	0.488
$\text{YAl}_3\text{B}_4\text{O}_{12}:\text{Ce}$	2.946	0.938	3.590	0.513
$\text{YBO}_3:\text{Ce}$	3.269	0.609	3.189	0.464
$\text{CaYAl}_3\text{O}_7:\text{Ce}$	2.508	0.759	2.876	0.435
$\text{LiYF}_4:\text{Ce}$	4.648	0.586	4.024	0.347
$\text{CaF}_2:\text{Ce},\text{F}$	4.375	0.537	3.863	0.368
$\text{CaAl}_4\text{O}_7:\text{Ce},\text{Na}$	2.908	0.692	3.203	0.431
$\text{CaSrAl}_2\text{SiO}_7:\text{Ce},\text{Na}$	2.673	1.014	2.748	0.542
$\text{Sr}_2\text{Al}_2\text{SiO}_7:\text{Ce},\text{Na}$	2.837	0.909	2.989	0.515
$\text{LiBaPO}_4:\text{Ce},\text{Na}$	3.374	0.673	2.709	0.514
$\text{Sr}_3\text{B}_2\text{O}_6:\text{Ce},\text{Na}$	2.900	0.616	2.866	0.432

Table S5. Statistical analyses of ΔSCF emission energy $\epsilon_{\text{em}}^{\Delta\text{SCF}}$ against calculated emission peak energy $\epsilon_{5/2}^{\text{cal}}$ and ΔSCF emission band FWHM against calculated emission FWHM $w_{5/2}^{\text{cal}}$ at 300 K. ME (eV), MAE (eV), MRE (%) and MARE (%) stand for the mean error, mean absolute error, mean relative error, and mean absolute relative error, respectively. The slope, intercept and coefficient of determination (R^2) correspond to the linear fitting. The number in parentheses indicates the standard deviation.

	$\epsilon_{5/2}^{\text{cal}}$ vs $\epsilon_{\text{em}}^{\Delta\text{SCF}}$	$w_{5/2}^{\text{cal}}$ vs $w_{\text{em}}^{\Delta\text{SCF}}$
ME (eV)	−0.03(20)	−0.06(11)
MAE (eV)	0.16(11)	0.07(10)
MRE (%)	0(6)	−8(18)
MARE (%)	5(3)	13(14)
Slope	1.07(10)	0.77(14)
Intercept (eV)	−0.25(33)	0.06(8)
R^2	0.91	0.76

Table S6. Statistical analysis of peak energy E_{em} and FWHM W_{em} of whole emission spectra of Ce^{3+} -activated phosphors calculated by FPMD spectra accumulation method. ME (eV), MAE (eV), MRE (%) and MARE (%) stand for the mean error, mean absolute error, mean relative error, and mean absolute relative error, respectively. The slope, intercept (eV) and coefficient of determination (R^2) correspond to the linear fitting. The number in parentheses indicates the standard deviation.

	E_{em}	W_{em}	$W_{\text{em}} - \Delta_{\text{SO}}$
ME	0.07(37)	0.27(11)	0.18(11)
MAE	0.30(22)	0.27(11)	0.18(11)
MRE	2(12)	58(19)	113(65)
MARE	9(7)	58(19)	113(65)
Slope	1.31(22)	2.02(47)	2.02(47)
Intercept	−0.89(69)	−0.19(22)	0.00(8)
R^2	0.78	0.65	0.65

References

- [S1] V. Bachmann, C. Ronda, A. Meijerink, “Temperature Quenching of Yellow Ce^{3+} Luminescence in $\text{YAG}:\text{Ce}^{3+}$ ”, *Chem. Mater.* **2009**, *21*, 2077. <https://doi.org/10.1021/cm8030768>
- [S2] T. Tomiki, H. Ishikawa, T. Tashiro, M. Katsuren, A. Yonesu, T. Hotta, T. Yabiku, M. Akamine, T. Futemma, T. Nakaoka, I. Miyazato, “ Ce^{3+} Centres in YAlO_3 (YAP) Single Crystals”, *J. Phys. Soc. Jpn.* **1995**, *64*, 4442. <https://doi.org/10.1143/JPSJ.64.4442>
- [S3] A. Bril, G. Blasse, J. A. De Poorter, “Fast - Decay Phosphors”, *J. Electrochem. Soc.* **1970**, *117*, 346. <https://doi.org/10.1149/1.2407508>.
- [S4] Y.-K. Choi, P. Halappa, C. Shivakumara, V. Dubey, V. Singh, “Blue emitting Ce^{3+} -doped CaYAl_3O_7 phosphors prepared by combustion route”, *Optik* **2019**, *181*, 1113. <https://doi.org/10.1016/j.ijleo.2018.10.213>
- [S5] Y. Yokota, T. Yanagida, K. J. Kim, A. Yoshikawa, N. Kawaguchi, S. Ishizu, K. Fukuda, M. Nikl, M. Miyake, M. Baba, “Growth, optical properties and neutron responses of Ce^{3+} doped LiYF_4 single crystals”, in *2008 IEEE Nucl. Sci. Symp. Conf. Rec.*, **2008**, pp. 1236–1239. <https://doi.org/10.1109/NSSMIC.2008.4774629>
- [S6] M. Uy, K. Shinohara, M. J. F. Empizo, T. Shimizu, M. Yoshimura, N. Sarukura, A. Yoshikawa, H. Abe, “Evidence of Undistorted 8-Coordinated Cubic (O_h) Ce^{3+} Center in Moderately-Doped (0.01 mol %) CaF_2 Single Crystal”, *J. Phys. Soc. Jpn.* **2022**, *91*, 124713. <https://doi.org/10.7566/JPSJ.91.124713>
- [S7] D. Jia, R. S. Meltzer, W. M. Yen, W. Jia, X. Wang, “Green phosphorescence of through persistence energy transfer”, *Appl. Phys. Lett.* **2002**, *80*, 1535. <https://doi.org/doi:10.1063/1.1456955>
- [S8] S. Miao, Z. Xia, M. S. Molokeev, J. Zhang, Q. Liu, “Crystal structure refinement and luminescence properties of blue-green-emitting $\text{CaSrAl}_2\text{SiO}_7:\text{Ce}^{3+}, \text{Li}^+, \text{Eu}^{2+}$ phosphors”, *J. Mater. Chem. C* **2015**, *3*, 8322. <https://doi.org/10.1039/C5TC01629K>
- [S9] T. Richhariya, N. Brahme, D. P. Bisen, Y. Patle, E. Chandrawanshi, N. Shah, “Luminescence properties of blue-emitting Ce^{3+} -doped series of $\text{Ca}_2\text{Al}_2\text{SiO}_7$ and $\text{Sr}_2\text{Al}_2\text{SiO}_7$ phosphors”, *J. Mater. Sci. Mater. Electron.* **2021**, *32*, 20793. <https://doi.org/10.1007/s10854-021-06593-z>
- [S10] D. Wei, Y. Huang, S. Zhang, Y. M. Yu, H. J. Seo, “Luminescence spectroscopy of Ce^{3+} -doped ABaPO_4 ($A=\text{Li}, \text{Na}, \text{K}$) phosphors”, *Appl. Phys. B* **2012**, *108*, 447. <https://doi.org/10.1007/s00340-012-4969-x>
- [S11] X. Li, C. Liu, L. Guan, W. Wei, Z. Yang, Q. Guo, G. Fu, “An ideal blue $\text{Sr}_3\text{B}_2\text{O}_6:\text{Ce}^{3+}$ phosphor prepared by sol-combustion method”, *Mater. Lett.* **2012**, *87*, 121. <https://doi.org/10.1016/j.matlet.2012.07.094>